A NOVEL ACQUISITION APPROACH FOR HEAT TRANSFER COEFFICIENT DURING PERIODIC COOLING PROCESS

by

Demin CHEN*, Zihuai HE, Yibo ZHAO, and Biao LU

School of Civil Engineering and Architecture, Anhui University of Technology, Ma'anshan, Anhui, China

Original scientific paper
https://doi.org/10.2298/TSCI211211035C

Temperature is an important parameter affecting the micro-structure of slab and an important guarantee to improve the performance index of metallurgical products. However, the temperature level is affected by the heat transfer coefficient. Taking laminar cooling as an example, a method for calculating the heat transfer coefficient of a system with periodic characteristics is proposed in this study. Firstly, it was assumed that the distribution of heat transfer coefficient is a piecewise function composed of positive half wave of sine function and line function. The calculation methods of characteristic parameters, through structural parameters and operating parameters, in three cases of "separation", "adjacent" and "intersection" are given. Secondly, heat transfer model of slab was established. Surface temperature and center temperature distribution of slab were compared with the test results. The relative errors of surface and center temperature were 2.46% and 1.33%, respectively, which verified the accuracy of this method. Finally, the coupling relationship between the characteristic parameters in the heat transfer coefficient distribution function is obtained by calculation. Compared with the methods presented in the literature, this method reduces the number of unknown parameters while ensuring the accuracy of the model, and gives guidance on how to change the slab temperature and improve product performance by adjusting the structure and operating parameters.

Key words: *heat transfer coefficient, periodic cooling, positive half wave, characteristic parameters, coupling relationships*

Introduction

With energy shortage and environmental load increasing, energy conservation and emission reduction and sustainable development have become global obligations and responsibilities [1-4]. Iron and steel industry has attracted extensive attention [5], which is high energy consumption [6, 7] and high emission [8-10]. Energy consumption of iron and steel industry accounts for 10-15% of the total energy consumption in the world, and the CO_2 emission accounts for about 7% of the total anthropogenic CO_2 emission [11]. In China, the total energy consumption of iron and steel industry was 609.34 Mtce (millionn coal equivalent), which accounted for about 20.18% of the total industrial energy consumption in 2018 landing at the top. Moreover, the iron and steel industry has been facing serious overcapacity [12, 13]. According to the statistics of World Steel Association, the global crude steel capacity utilization rate was 69.0% in 2016. Meanwhile, China's crude steel capacity utilization was 74% during this period

* Corresponding author, e-mail: cdm780823@163.com

[14]. Because of the aforementioned reasons, it is necessary to further develop products with high value-added and high quality due to survival and development of iron and steel enterprises [15-17]. This means that the temperature field of metal materials, which affects the processability of final products, become an important research content. The main processes of changing slab temperature in casting rolling system include dephosphorization, laminar cooling, cooling between rolling mill*, etc.* which have obvious periodic characteristics. Laminar cooling system (LCS) is a typical among them.

The LCS is the main way to realize slab rapid cooling in hot rolling strips [18-21]. In this process, slab cooling is divided into two areas, one is air cooling, and the other is water cooling. In the air cooling, convection and radiation are the main heat transfer modes, which occur between the slab surface and the air. In the water cooling, convection is the main heat transfer mode, which can be divided into two regions (impinging zone and non-impinging zone) after the cooling water impinges on the slab surface [22]. In impinging zone, single-phase forced convection is the main heat transfer mode. Obviously, the slab surface temperature decreases rapidly due to the strong heat exchange between slab surface and cooling water. However, the slab internal temperature is still high due to time limitation of heat transfer process. Therefore, there will be a large temperature gradient between surface and inside of the slab. In non-impinging zone, boiling heat transfer is the main heat transfer mode. Quite evidently, heat transfer process is weakened between slab surface and cooling water in non-impinging zone.

During the cooling process, the micro-structure of the metal formed by the decomposition and precipitation of austenite is closely related to the temperature distribution, level and gradient [20, 23]. While heat transfer boundary directly affect and determine the temperature distribution. Consequently, it is important to study on the heat transfer coefficient (HTC) distribution pattern. However, it is difficult to be estimated by simple methods [24, 25], due to the heat transfer mechanism of hot rolling strips in the LCS is complex. Presently, the methods to obtain the HTC mainly include: experimental method, empirical method, semi empirical method.

Experimental method is to obtain the HTC by inverse heat transfer algorithm based on the measured slab temperature field data. Some scholars [26-29] designed experiment platforms for analyzing the effects of different water flows, water temperature, nozzle interval, nozzle height*, etc.* on cooling rate. Then, the conjugate method was used to establish the inverse heat conduction problem model to achieve the cooling surface temperature, HTC and other parameters, as well as the boundary conditions. The HTC distribution obtained by this method reflects the comprehensive results of structural parameters and operating parameters. It cannot give guidance to change the temperature field of slab by adjusting the structure or operating parameters.

Empirical formula method refers to the complete expression of the HTC obtained from literature, which is often used in numerical calculation [30-33]. Yi *et al*. [23] established the 2-D slab heat transfer model, in which HTC was achieved by empirical formula from literature. The number of cooling water header groups and the water flux of each header group were taken as control variables to adjust the temperature distribution of the strip. Jiang [34] obtained the strip temperature trends for various strip thicknesses and ultra-fast cooling rates by numerical calculation method. Re-reddening temperature, temperature deviation between surface and center, and boundary-layer position changing law were also obtained. Meanwhile, the HTC has been achieved by empirical formula. Empirical formula has certain applicable conditions. When the calculation conditions exceed the applicable range, the calculation accuracy of the model will be affected.

The semi empirical formula method refers to the general expression of the HTC obtained from literature, and the coefficient is modified according to the historical data of the research object. Yu [35] used back propagation neural work combined with mathematical model to work out the HTC of LCS of hot continuous rolling in water cooled region. The standard deviation between the predicted and measured coiling temperature reduce 22.84%. Xie [36] optimized the parameters of air/water cooling models by regressing the data gathering in situ, and satisfactory effect was obtained. The coiling temperature can be controlled within ±15 ℃. Compared with the empirical formula method, the semi empirical method increases the calculation accuracy of the slab temperature field model, and the slab temperature field can be adjusted by changing the parameters according to the influencing factors contained in the formula. However, the problem of this kind of method is that when there are many unknown parameters contained in the formula, the accuracy after fitting will be affected.

In these studies, different research methods are used to obtain the HTC. However, there is one thing in common, that is they have no in-depth analysis of the common characteristics of the HTC in periodic cooling process. Characteristic parameters of periodic function reflect the common characteristics of a kind of process, not just one. In this study, a method for obtaining the HTC of periodic cooling process is presented. Novelty of the method is mainly reflected in: first, the distribution form of HTC is given first through process analysis, which is a piecewise function composed of half wave sine and linear function; Secondly, characteristic parameters in the piecewise function can be calculated by structural parameters or operating parameters, which reduces the unknowns in the empirical formula. Thirdly, the obtained HTS distribution function can provide guidance for adjusting the slab temperature by changing the slab structure or operating parameters. Although less operating parameters are involved, it provides a way to change slab micro-structure and improve product quality. The method presented by this study not only simplifies the solving process, but also provides a general method to calculate the HTC for the production process which have the same characteristics.

Methodologies

Heat transfer model of slab

It is assumed that the temperature along the width direction of the slab is evenly. Meanwhile, because of large width-to-thickness ratio of the slab, the heat transfer between the external environment and the slab upper and lower surfaces are considered, while the sides of the slab are considered to be adiabatic.

The differential equation of heat conduction in slab is established [37]:

$$\rho c_p \frac{\partial T}{\partial \tau} = \frac{\partial}{\partial x}\left(\lambda \frac{\partial T}{\partial x}\right) + \frac{\partial}{\partial y}\left(\lambda \frac{\partial T}{\partial y}\right) \tag{1}$$

where x, y [m] are the co-ordinate along slab width and height, ρ [kgm^{-3}] – the slab density, λ [Wm^{-1}℃$^{-1}$] – the slab thermal conductivity, and c_p [kJkg^{-1}℃$^{-1}$] – the slab heat capacity.

Then, the slab thermal conductivity should be corrected according to temperature. Meanwhile, the slab heat capacity should also be corrected according to temperature. The correction methods are shown in [38].

The initial conditions:

$$T(x, y) = T_c \quad (0 < x < b; \quad 0 < y < H) \tag{2}$$

where T_c [℃] is the slab initial temperature, b [m] – the slab width, and H [m] – the slab thickness.

The boundary condition is the third kind of heat transfer:

$$-\lambda \frac{\partial T(y,\tau)}{\partial y}|_{y=H_c} = h_c(T_w - T_s) \tag{3}$$

where h_c [Wm^{-2}°C^{-1}] is the HTC in the LCS, T_w [°C] – the surface temperature of the slab, and T_s [°C] – the cooling medium temperature of the LCS. It is the air temperature in the air cooling, while it is the water temperature in the water cooling.

It should be noted that the slab conduction governing differential equation is discretized by the finite volume method, and the additional source term method is adopted in treatment of boundary condition. Then, alternative direction implicit iteration has been applied to calculate slab temperature field.

Acquisition of the HTC in LCS

Distribution function of the HTC

The LCS area can be divided into several local regions, which centered on each row of nozzles. Additionally, the cooling water is sprayed downward at an angle through row of nozzles in each local region. According to the spray shape of cooling water, the HTC of slab surface can be assumed as a sinusoidal function or line function in each local region. Then, the relative position of sinusoidal function between adjacent local regions is affected by the nozzle spacing and slab running speed. There are three possible states

Firstly, the relevant variable should be introduced. The B [m] is the nozzle spacing, v_c [ms^{-1}] is th slab running speed, φ_c [s] is the quarter period of sine curve, and φ_0 [s] is the time interval between two adjacent sinusoids:

– *Disjoint*

Disjoint will be happened when $\varphi_c < B/(2v_c)$. Therefore, HTC can be expressed as a combination of sinusoidal and linear functions, as shown in fig. 1. Take n^{th} local region as an example, the HTC:

$$h_{c,n} = \begin{cases} h_{c,n,L} & \dfrac{(2n-3)B}{2v_c} < \tau \le \left[(2n-3)\varphi_c + (n-1)\varphi_0\right] \\ h_{c,n,s} & \left[(2n-3)\varphi_c + (n-1)\varphi_0\right] < \tau \le \left[(2n-1)\varphi_c + (n-1)\varphi_0\right] \\ h_{c,n,R} & \left[(2n-1)\varphi_c + (n-1)\varphi_0\right] < \tau \le \left[(2n-1)\varphi_c + \dfrac{(2n-1)}{2}\varphi_0\right] \end{cases} \tag{4}$$

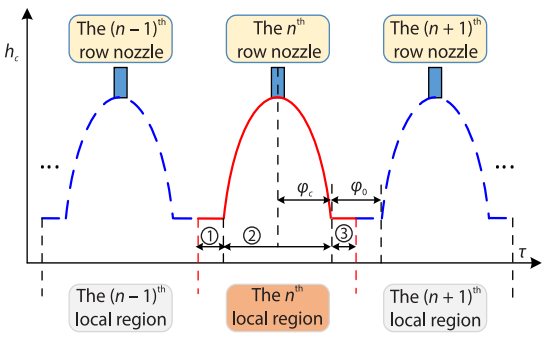

Figure 1. The distribution of HTC in *Disjoint* state

where $h_{c,n}$ [Wm^{-2}°C^{-1}] is the HTC in n^{th} local region, $h_{c,n,L}$ [Wm^{-2}°C^{-1}] – the HTC in section ① (fig. 1) of n^{th} local region, $h_{c,n,L} = h_{c,n,\,L,co} + h_{c,n,L,ra}$, $h_{c,nL,co}$ are the HTC in section ① of n^{th} local region, $h_{c,n,L,co} = 2.15(T_{w,n,L} - T_s)^{1/4}$, $h_{c,n,L,ra}$ – the radiation HTC in section ① of n^{th} local region, $h_{c,n,L,ra} = \sigma\varepsilon[(T_{w,n,L} + 273) + (T_s + 273)][(T_{w,n,L} + 273)^2 + (T_s + 273)^2]$, σ – the black-body radiation constant, $5.67\cdot10^{-8}$ W/(m^{2}K^4), ε – the lab surface emissivity, $T_{w,nL}$ [°C] – the slab surface temperature of n^{th} local region

in left, $h_{c,n,R}$ [Wm^{-2}°C^{-1})] – the HTC in section ③ of n^{th} local region. The computing method of the $h_{c,n,R}$ is the same as $h_{c,n,L}$. The $h_{c,n,s}$ [Wm^{-2}°C^{-1}] is the HTC in section ② of n^{th} local region, $h_{c,n,s} = A_c \sin(\omega_c\{\tau - [(2n-3)\varphi_c + (n-1)\varphi_0]\})$. The A_c [Wm^{-2}°C^{-1})] is the amplitude of sinusoidal function and ω_c [rads^{-1}] – the angular frequency of sinusoidal function.

– *Adjacent*

Adjacent will be happened when $\varphi_c = B/(2v_c)$. Therefore, HTC can be expressed as a sinusoidal functions, as shown in fig. 2. Take n^{th} local region as an example yet, the HTC:

$$h_{c,n} = A_c \sin\left\{\omega_c\left[\tau - (2n-3)\varphi_c\right]\right\}, \quad (2n-3)\varphi_c < \tau \le (2n-1)\varphi_c \tag{5}$$

– *Cross*

Cross will be happened when $\varphi_c = B/(2v_c)$. Therefore, HTC can be expressed as a sinusoidal functions, as shown in fig. 3. Take n^{th} local region as an example yet, the HTC:

$$h_{c,n} = A_c \sin\left(\omega_c\left\{\tau - \left[(2n-3)\varphi_c - (n-1)\varphi_0\right]\right\}\right)$$
$$\left[(2n-3)\varphi_c - \frac{(2n-3)}{2}\varphi_0\right] < \tau \le \left[(2n-1)\varphi_c - \frac{(2n-1)}{2}\varphi_0\right] \tag{6}$$

In short, the HTC is composed of sinusoidal or linear functions along the direction

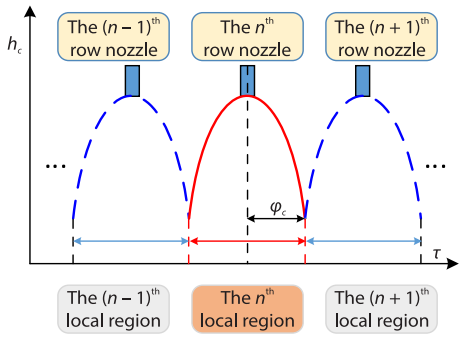

Figure 2. The distribution of HTC in *Adjacent* state

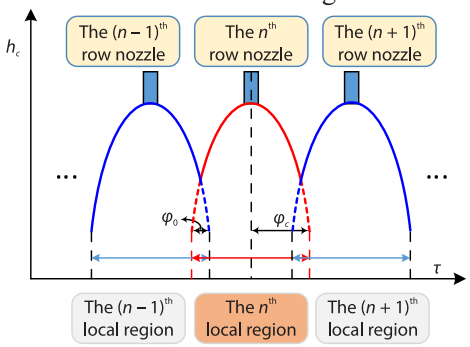

Figure 3. The distribution of HTC in *Cross* state

of slab movement. The heat transfer intensity in linear function region is much weaker than in sinusoidal function region. Therefore, sinusoidal function region will be discussed in the following section.

The characteristic parameters of the distribution function of the HTC

The characteristic parameters of sinusoidal function include A_c, ω_c, and φ_c, as shown in eqs. (4)-(6). Next, how to obtain these characteristic parameters from structural parameters, operating parameters and experimental data is described:

– The calculation of ω_c

Take the n^{th} row nozzle as an example, as shown in fig. 4, the ω_c can be calculated through structural parameters of the LCS and slab running speed (operating parameter).

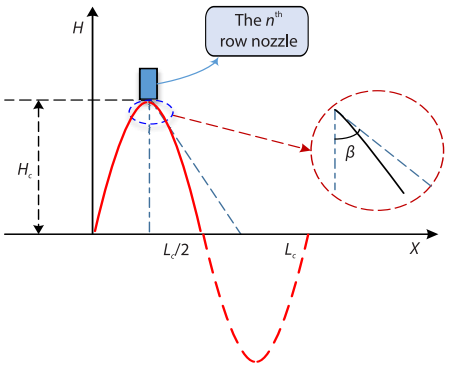

Figure 4. The sinusoidal function wavelength of the n^{th} row nozzle

The relevant parameters in fig. 4 are described v_c [ms^{-1}] is the slab running speed, β – the spray angle of the n^{th} row nozzle, [0, L_c/2] – the actual water cooling length with sinusoidal function (solid line) in the n^{th} row nozzle, [L_c/2, L_c] – the virtual water cooling length with sinusoidal function (dotted line) in the n^{th} row nozzle, [0, L_c] – full water cooling length with sinusoidal function in the n^{th} row nozzle, and L_c [m] – the full water cooling length with sinusoidal function in the n^{th} row nozzle.

Generally, the sinusoidal function curve in the range of [0, L_c/4] is approximately a straight line. Then T_c can be calculated:

$$T_c = \frac{L_c}{v_c} = \frac{4H_c \tan\beta}{v_c} \tag{7}$$

where T_c is the sinusoidal period when slab passes through the range of [0, L_c] at the speed v_c [ms^{-1}].

– The calculation of φ_0 and φ_c

The φ_0 and φ_c determine the initial phase of sinusoidal function. The φ_c is a quarter of the period of the sine function. The calculation formula:

$$\varphi_c = \frac{T_c}{4} = \frac{H_c \tan\beta}{v_c} \tag{8}$$

Then, the value of φ_0 depends on the relative position of φ_0 and φ_c.

Disjoint:

$$\varphi_0 = \frac{B - 2H_c \tan\beta}{v_c} = 2\left(\frac{B}{2v_c} - \varphi_c\right) \tag{9}$$

Adjacent:

$$\varphi_0 = 0 \tag{10}$$

Cross:

$$\varphi_0 = \frac{2H_c \tan\beta - B}{v_c} = 2\left(\varphi_c - \frac{B}{2v_c}\right) \tag{11}$$

– The calculation of A_c

The amplitude, A_c, of sinusoidal function is affected by nozzle height, flow velocity and spray angle. However, the quantitative relationship between A_c and these structural parameters is ambiguous. Consequently, test data and structure dimension data of the experiment platform can be fully utilized. More concretely, the appropriate A_c can be achieved through comparing slab temperature field test data with the heat transfer model calculation data. Essentially, it is an optimization process.

Objective function of optimization:

$$\min \sum_{i=1}^{n} \left(x_i - x_i'\right)^2 \tag{12}$$

where n is the number of detected data points, x_i – the i^{th} moment temperature calculated by heat transfer model, and x_i' – the i^{th} moment temperature detected by experiment platform.

Constraint equation:

$$A_c > 0 \tag{13}$$

Thus, the aforementioned parameters, ω_c, φ_0, φ_c, and A_c, have been calculated. Then, the HTC of any relative relation can be achieved.

Method validation

According to eqs. (4)-(6), the characteristic parameters of HTC mainly include: angular frequency of sinusoidal function, ω_c, initial phase, φ_0 and φ_c, and sine amplitude, A_c. The LCS platform, which can validate the effectiveness of method, have been established in this study.

The slab size, structure size and slab running speed used in the experiment are shown in fig. 5. The length of the cooling zone in the experimental platform is 2160 mm.

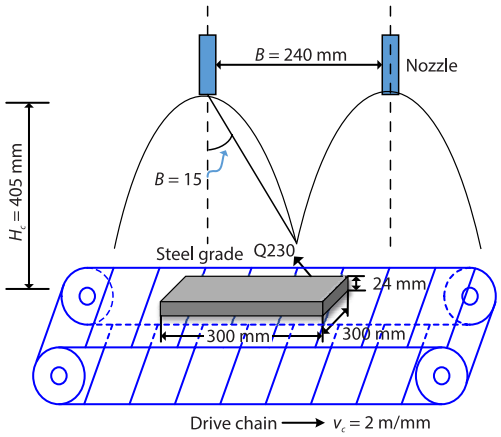

Figure 5. Parameters in the experiment

The surface temperature (ST) and center temperature (CT) are measured at the position of 1 mm and 13 mm away from the surface, respectively. Three points are selected for ST measurement and two points are selected for CT measurement. The positions of the ST measuring points are determined by average dividing the width after removing 5 mm of the front and rear edges, respectively. The positions of the CT measuring points are determined by average dividing the width. During the experiment, the thermocouple was welded in the test position by drilling, and then filled with refractory mud.

Cold experiment on nozzle spray angle has been carried out. The experimental results show that nozzle spray angle, $\beta = \pi/12$. Therefore, ω_c, φ_0, and φ_c can be calculated. Position relationship between nozzles can be considered as *Disjoint*. The H_c distribution in the water cooling area is shown in fig. 6.

The ST and CT of slab obtained by model and experiment are shown in fig. 7

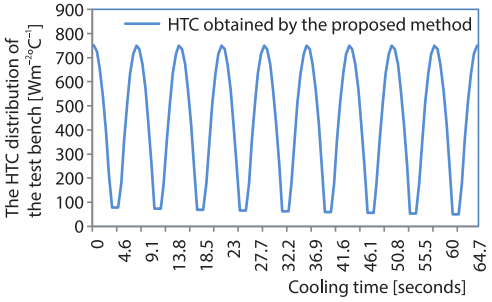

Figure 6. The HTC distribution along the cooling direction

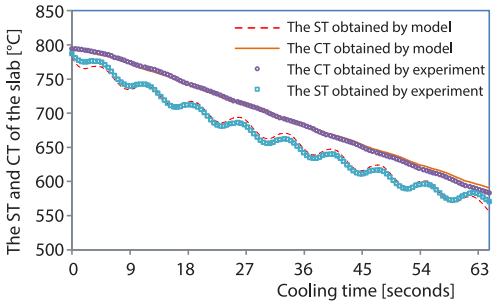

Figure 7. The ST and CT of the slab

For ST of the slab, the relative error between the measured value and the model calculation value is 2.46%. For CT of the slab, the relative error between the measured value and the model calculation value is 1.33%. It can be concluded that the method to obtain the HTC proposed in this study is feasible.

Co-ordination among the characteristic parameters of HTC

The method to obtain the HTC of laminar cooling is given in the previous of this study, and the accuracy of this method is verified by experiments. Then there is another problem that is most concerned in practical engineering. Metal material cooling process is often to control the

end temperature to meet the next technological setting requirements. In order to satisfy the end temperature, there will be a variety of cooling schemes, which are shown that the characteristic parameters of HTC changes co-operatively in the heat transfer problem. Therefore, this study makes a more in-depth analysis based on the previous experimental model.

The characteristic parameters of HTC include sine amplitude, angular frequency (or sine period) and initial phase. The size of the sine initial phase is limited with the position of the nozzle. So the sine initial phase and the sine period are correlation variables. The actual independent characteristic parameters are sine amplitude and sine period. Period is affected by the nozzle height and the slab running speed, as shown in eq. (7). In order to analyze the problem conveniently, the slab running speed is converted into the cooling time, which can be solved by the cooling zone length divided by the cooling speed. Therefore, the analysis of the characteristic parameters of the HTC mainly includes co-ordination among the nozzle height, sine amplitude and cooling time of the HTC.

In order to obtain the co-ordination, an optimization model of the slab was established. Objective function can be expressed:

$$\min(t_{c,e} - t_{c,0}) \tag{14}$$

where $t_{c,e}$ [°C] is coiling temperature calculated by model and $t_{c,0}$ [°C] – the arget cooling temperature of the slab.

The decision variables in the optimization function are the slab running speed (or the nozzle height) and amplitude according to different research contents.

Constraints:

$$\tau \in (\tau_{\min}, \tau_{\max}) \tag{15}$$

$$H_c > 0 \tag{16}$$

where $\tau_{\min}$ and $\tau_{\max}$ [min] are the minimum and maximum cooling time of a certain type of steel in normal production.

The optimization model is solved by sequential quadratic programming algorithm. The solving process is realized by the fmincon function of MATLAB.

This study takes the heat transfer model, which is established on the aforementioned method for experimental platform, to introduce the co-ordination among the nozzle height, sine amplitude and cooling time of HTC.

The range of the slab running speed is 1~5 m/min in the experiment. The length of the cooling zone in the experimental platform is 2160 mm. So the cooling time range is 25.90~129.60 seconds. The range of the nozzle height is 365~565 mm. In previous-mentioned range, 0.1 second and 20 mm are taken as the steps of cooling time and nozzle height, respectively to carry out optimization calculations. The sine amplitudes in certain conditions are obtained, respectively. The function relationship among the nozzle height, the sine amplitude and the cooling time can be obtained:

$$A_c = -180.34 + 12188.17\tau_c^{(-0.77)} H_c^{(-0.77)} \tag{17}$$

The functional relationship between sine amplitude and period can be obtained by taking eqs. (7)-(17) as:

$$A_c = -180.34 + 7147.36T_c^{-0.77} \tag{18}$$

Conclusions

In this study, the distribution of HTC along the running direction of slab is characterized. The characteristic parameters can be calculated by structural parameters or operating pa-

rameters, which reduces the unknowns in the empirical formula. While ensuring the calculation accuracy of the model, the methods of changing the temperature field through the adjustment of operating parameters and structural parameters are given. This provides a way for changing the micro-structure of slab and improving product quality. Specifically, the following conclusions can be drawn.

- Distribution of the HTC is a piecewise function composed of positive half wave of sine function and line function. The general distribution forms of HTC in *Disjoint*, *Adjacent* and *Cross* are obtained
- The characteristic parameters of the HTC include sine period, initial phase and sine amplitude, whereas the initial phase is affected by the period. Their values can be calculated by structural parameters, operating parameters and experimental data.
- The method to obtain the HTC has been verified by experiment platform. For slab ST, the relative error between the measured value and the model calculation value is 2.46%. For slab CT, the relative error between the measured value and the model calculation value is 1.33%. Therefore, the calculation method of HTC fully meets the accuracy requirements in LCS area.
- Based on the HTC distribution obtained by this study, the co-ordination relationship among the sine amplitude, nozzle height and cooling time are obtained.

Acknowledgment

Project supported by the National Natural Science Foundation of China (NO. 51804002) and by the National Key Research and Development Program (Project No. 2020YFB1711101). The authors gratefully acknowledge the reviewers and editors for their fruitful comments.

References

[1] Xuying, W., *et al*., A Unit-Based Emission Inventory of SO_2, NO_x and PM for the Chinese Iron and Steel Industry from 2010 to 2015, Science o*f the Total Environment*, *676* (2019), 7521, pp. 18-30
[2] Chengkang, G., *et al.*, Comprehensive Evaluation on Energy-Water Saving Effects in Iron and Steel Industry, *Science of the Total Environment*, *670* (2019), June, pp. 346-360
[3] Kazuaki, Y., *et al*., Optimization of Thermoelectric Topping Combined Steam Turbine Cycles for Energy Economy, *Applied Energy*, *109* (2013), Sept., pp. 1-9
[4] Bing, X., *et al*., Modelling and Performance Analysis of a Two-Stage Thermoelectric Energy Harvesting System from Blast Furnace Slag Water Waste Heat, *Energy*, *77* (2014), Dec., pp. 562-569
[5] Changxin, L., *et al*., System Dynamics Analysis on Characteristics of Iron-Flow in Sintering Process, *Applied Thermal Engineering*, *82* (2015), May, pp. 206-211
[6] Lu, B., *et al.*, An All-Factors Analysis Approach on Energy Consumption for the Blast Furnace Iron Making Process in Iron and Steel industry, *Processes*, *607* (2019), 7, 607
[7] Lu, B., *et al*., An Energy Intensity Optimization Model for Production System in Iron and Steel Industry, *Applied Thermal Engineering*, *100* (2016), May, pp. 285-295
[8] Jia, J., *et al*., Emission Characteristics and Chemical Components of Size-Segregated Particulate Matter in Iron and Steel Industry, *Atmospheric Environment*, *182* (2018), June, pp. 115-127
[9] Haozhe, Y., *et al*., The Contribution of the Beijing, Tianjin and Hebei Region's Iron and Steel Industry to Local Air Pollution in Winter, *Environmental Pollution*, *245* (2019), Feb., pp. 1095-1106
[10] Qi, Z., *et al*., Optimization of Energy use with CO_2 Emission Reducing in an Integrated Iron and Steel Plant, *Applied Thermal Engineering*, *157* (2019), 113635
[11] Chen, L. G., *et al.*, Thermodynamic Optimization Opportunities for the Recovery and Utilization of Residual Energy and Heat in China's Iron and Steel Industry: A Case Study, *Applied Thermal Engineering*, *86* (2015), July, pp. 151-160
[12] Zhaoling, L., *et al*., Assessment of the Carbon Emissions Reduction Potential of China's Iron and Steel Industry Based on a Simulation Analysis, *Energy*, *183* (2019), Sept., pp. 279-290
[13] Lu, B., *et al*., A Novel Approach for Lean Energy Operation Based on Energy Apportionment Model in Reheating Furnace, *Energy*, *182* (2019), Sept., pp. 1239-1249

[14] ***, China Iron and Steel Association, China Steel Annual Development Report (in Chinese), China Iron and Steel Association, Beijing, China, 2017, pp. 29-30
[15] Zongguo, W., *et al*., Quantitative Analysis of the Precise Energy Conservation and Emission Reduction Path in China's Iron and Steel Industry, *Journal of Environmental Management*, *246* (2019), Sept., pp. 717-729
[16] Hai-Ling, L., *et al.*, Environmental Regulations, Environmental Governance Efficiency and the Green Transformation of China's Iron and Steel Enterprises, *Ecological Economics*, *165* (2019), 106397
[17] Shu-Hua M., *et al.*, Mode of Circular Economy in China's Iron and Steel Industry: A Case Study in Wu'an City, *Journal of Cleaner Production*, *64* (2014), Feb., pp. 505-512
[18] Gong, D.-Y., *et al*., Self-Learning and Its Application Laminar Cooling Model of Hot Rolled Strip, Journal of Iron and Steel Research, *International*, *14* (2007), 4, pp. 11-14
[19] Xie, H. B., *et al*., Application of Fuzzy Control of Laminar Cooling for Hot Rolled Strip, *Journal of Materials Processing Technology*, *187-188* (2007), June, pp. 715-719
[20] Jinxiang, P., *et al*., A Hybrid Soft Sensor for Measuring Hot-Rolled Strip Temperature in the Laminar Cooling Process, *Neurocomputing*, *169* (2015), Dec., pp. 457-465
[21] Peng, L., *et al*., Mathematic Modelling on Flexible Cooling System in Hot Strip Mill, *Journal of Central South University*, *21* (2014), Mar., pp. 43-49
[22] Han, B., *Research on Modelling and Control for Laminar Cooling in Hot Strip Mill* (in Chinese), Norteasterm University, Shenyang, China, 2005, pp. 11, 19
[23] Yi, Z., *et al.*, Distributed Model Predictive Control for Plant-Wide Hot-Rolled, *Journal of Process Control*, *19* (2009), 9, pp. 1427-1437
[24] Zhang, D.-H., *et al*., Cooling Efficiency of Laminar Cooling System for Plate Mill, Journal of Iron and Steel Research, *International*, *15* (2008), 5, pp. 24-28.
[25] Liu, E.-Y., *et al.*, Algorithm Design and Application of Laminar Cooling Feedback Control in Hot Strip Mill, Journal of Iron and Steel Research, *International*, *19* (2012), 4, pp. 39-42
[26] Wang, M. T., *et al*., Experimental Study on the Laminar Cooling Process of the Middle and Heavy Plate, *Applied Mechanics and Materials*, *232* (2012), Nov., pp. 808-811
[27] Wen-Hong, L., *et al*., Mathematical Modelling and Experimental Study of Inverse Heat Conduction Problems of Heavy Plate Laminar Cooling Process, *Advances in Computer Science Research*, *54* (2016), Dec., pp. 408-412
[28] Wen-Hong, L., *et al*., Experimental Study and Application of Process Control on Hot Strip Mill's Laminar Cooling System, *Advances in Computer Science Research*, *52* (2016), Dec., pp. 513-516
[29] Yipeng, L., Laminar Cooling Experiment of Moving Plate at High Temperature and Study on Calculation Based on Inverse Heat (in Chinese), M. Ph. thesis of Engineering, Shanghai Jiao Tong University, Shanghai, China, 2009, Vol. 5, pp. 11-26
[30] Han, B., *et al*., Flow Field Simulation in Header Pipe of Laminar Cooling System for Hot Rolling and Theoretical Calculation of Impact Pressure, *Journal of Iron and Steel Research*, *16* (2004), 5, pp. 42-46
[31] Zhu, Q., *et al*., Numerical Simulation of Transient Temperature Field of Steel Plate Cooled with Circular Laminar Jets after Rolling (in Chinese), *Transactions of Mat. and Heat Treatment*, *25* (2004), 2, pp. 72-75
[32] Nobari, A. H., *et al.*, Modelling of Heat Transfer during Controlled Cooling in Hot Rod Rolling of Carbon Steels, *Applied Thermal Engineering*, *31* (2011), 4, pp. 487-492
[33] Edalatpour, S., *et al*., Effect of Phase Transformation Latent Heat on Prediction Accuracy of Strip Laminar Cooling, *Journal of Materials Processing Technology*, *211* (2011), 11, pp. 1776-1782
[34] Jiang, L.-Y., *et al*., Hot Rolled Strip Re-reddening Temperature Changing Law during Ultra-fast Cooling, *Journal of Iron and Steel Research, International*, *22* (2015), 8, pp. 694-702
[35] Yu, Q.-B., *et al.*, Solving Heat transfer Coefficient of Laminar Cooling by Neutral Networks (in Chinese), *Journal of Northeastern University (Natural Science)*, *23* (2002), 6, pp. 573-576
[36] Xie, H.-B., *et al*., Optimization and Model of Laminar Cooling Control Thickness Measurement System for Hot Strip Mills, Journal of Iron and Steel Research, *International*, *13* (2006), 1, pp.18-22
[37] Sang, H. H., *et al*., Efficiency Analysis of Radiative Slab Heating in a Walking-Beam-Type Reheating Furnace, *Energy*, *36* (2011), 2, pp. 1265-1272
[38] Li, H., *Study on Structural Parameters of Walking-beam Reheating Furnace Based on Zonal Method*, Wuhan University of Science and Technology, Wuhan, China, 2018, p. 37

Paper submitted: December 11, 2021
Paper revised: January 22, 2022
Paper accepted: January 24, 2022